Acta Cryst. (1993). B49, 745–754

A Study of Disorder in the SiO_2 Host Lattice of Dodecasil 1H using Synchrotron Radiation

BY G. MIEHE

Fachgebiet Strukturforschung, FB Materialwissenschaft, Technische Hochschule, Petersenstrasse 20, D-6100 Darmstadt, Germany

T. VOGT*

Institut Laue–Langevin, Grenoble CEDEX, France

H. FUESS

Fachgebiet Strukturforschung, FB Materialwissenschaft, Technische Hochschule, Petersenstrasse 20, D-6100 Darmstadt, Germany

AND U. MÜLLER†

Institut Anorganische und Analytische Chemie der Universität, D-6500 Mainz, Germany

(*Received* 22 *July* 1992; *accepted* 4 *February* 1993)

Abstract

Single-crystal diffraction data of dodecasil 1H (D1H), a clathrasil (SiO_2) with 1-aminoadamantane and NH_3 as guest molecules, were collected from a small crystal ($V = 2.5 \times 10^5$ μm^3) with synchrotron radiation (SR) ($\lambda = 0.78914$ Å) at the five-circle diffractometer of HASYLAB (DESY, Hamburg, Germany). The space group is *P6/mmm* with $a = 13.826\,(3)$, $c = 11.186\,(3)$ Å, $V = 1852\,(1)$ Å^3, the content of the unit cell is $34SiO_2(C_{10}H_{15}NH_2)5NH_3$, $F(000) = 1154$, $D_x = 2.043$ g cm^{-3}, $M_r = 2278.4$ g mol^{-1}. The structure refinement is based on 784 unique reflections ($R = 2.62\%$, $wR = 1.76\%$). The results are compared with studies using a conventional X-ray source. All O-atom sites were found to be split (average O—O distance 0.5 Å) indicating a disorder of the SiO_2 host framework. The mean Si—O distance, Si—O—Si angle and U_{eq} (oxygen) from anisotropic refinement without splitting were 1.568 Å, 170.7°, 0.065 Å^2, respectively, changed to 1.596 (11) Å, 155 (3)°, 0.038 (6) Å^2. Simulations based on distance least-squares calculations qualitatively match the results of the refinement. Additional data collected on a conventional diffractometer with monochromatized Mo $K\alpha$ radiation revealed only limited evidence for split O-atom positions. Anisotropic refinement of non-split O atoms with data collected at 155 K [$a = 13.748\,(3)$, $c = 11.128\,(3)$ Å] with Mo $K\alpha$ radiation gave only a minor decrease of the large O-atom r.m.s. amplitudes perpendicular to the direction of the Si—O bond. Population parameters > 1.0 for the O atoms obtained from refinement are shown to be an artefact inherent in the least-squares algorithm in the case of split sites. The 1-aminoadamantane guest molecule does not accommodate the symmetry of the host cage. Its threefold axis is inclined about 20° with respect to the sixfold axis of the cage.

Introduction

Recent single-crystal experiments using synchrotron radiation (SR) have demonstrated the feasibility of measuring reliable intensities from microcrystals (Rieck, Euler, Schulz & Schildkamp, 1988; Kupcik, 1988; Andrews *et al.*, 1988). But there is also a case for measuring 'big' crystals using SR rather than sealed X-ray tubes, namely if the accuracy of weak reflections is crucial for the structural work. One of these cases is accurate structure analysis for deformation-density studies. It was shown by Kirfel & Eichhorn (1990) that the reliability of weak reflections is increased substantially by experiments with SR. Thus the stability in refinements is increased and the noise in deformation-density maps is reduced. Cases where the accuracy of both weak and strong reflections is crucial are disordered molecules in either open cages, like in zeolites, or in closed cages, like in clathrate compounds. Here disorder may be observed in the host as well as in the guest structure.

We have measured intensities for dodecasil 1H (D1H), a clathrate with a silica framework (clathrasil) using SR. Preliminary results from these

* Present address: Physics Department, Brookhaven National Laboratory, Upton, New York 11973, USA.

† Present address: BASF, D-6700 Ludwigshafen, Germany.

measurements have been reported elsewhere (Miehe, Vogt, Müller & Fuess, 1990).

The content of the hexagonal unit cell is

$$34SiO_2 \cdot 3M^{12} \cdot 2M^{12'} \cdot M^{20}$$

where M^i is the content of an i-sided cage which is defined by the Si atoms as corners.

In D1H the SiO_4 tetrahedra are corner-linked to build a three-dimensional four-connected silica network: the basic building blocks of the structure are pentagondodecahedra (5^{12} cages, point symmetry *mmm*, three cages per unit cell) with a free diameter of roughly 5.7 Å. Each cage faces four others forming layers of hexagonal symmetry. These layers are connected *via* common O atoms and stacked with the sequence AA'. Two other types of cages are generated by this stacking, two $4^3 5^6 6^3$ cages (free diameter 5.7 Å, point symmetry $\bar{6}m2$) and one $5^{12}6^8$ cage (rotation ellipsoid with $d_1 = 7.1$, $d_2 = 11.2$ Å, point symmetry $6/mmm$) per unit cell. In the present study the latter cage hosts 1-aminoadamantane, whereas the small cages contain NH_3 molecules. The guest molecules entrapped in the cages cannot exchange in contrast to zeolites. Gerke & Gies (1984) first described the structure of D1H with piperidine and later Gies (1986) with 1-aminoadamantane and N_2 as guest molecules. Both these X-ray single-crystal studies were performed using a Philips PW 1100 automatic four-circle diffractometer. The structures of the SiO_2 host lattices were found to be identical within the limits of experimental error. Fig. 4(*b*) shows the asymmetric unit of this structure as obtained from the refinement of our data. There are, however, some rather problematic features:

(1) The mean Si—O distance of 1.568 Å (Gies, 1986) is much too short and the mean Si—O—Si angle of 170.5° is too close to 180° compared with the structures of other silica polymorphs showing no disorder. The mean value of the isotropic equivalent atomic displacement parameters (a.d.p.'s) is $U = 0.019$ Å^2 for the Si atoms but 0.065 Å^2 for the O atoms. The large O-atom a.d.p.'s the largest components of which are perpendicular to the directions of the Si—O bonds must be caused by some kind of disorder which should be studied in more detail. Liebau (1984) demonstrated that a significant bond shortening for SiO_2 framework structures is correlated with high values of the a.d.p.'s for the O atoms. Freimann & Küppers (1991) report elastic constants which are smaller by a factor of 3–4 than the ones calculated on the basis of the structure. Here also unreasonably large Si—O—Si angles [presumably Si(2)—O(4)—Si(2), which shares the *A* layers] lead to a higher rigidity than actually present. A recent study of calcined dodecasil 3C (D3C) with SR at 573 K (Könnecke, Miehe & Fuess, 1993) revealed a disorder of the O atoms.

(2) The position of the enclathrated molecules could not be determined precisely in the previous study. Therefore the host–guest interaction and a possible influence of the guest molecules on the symmetry of the framework cannot be discussed in detail.

The second question requires accurate intensities of strong reflections in the low-angle region. Therefore a small crystal should be used for data collection to minimize the influence of extinction.

To tackle the first point raised above well resolved electron densities are needed. Therefore accurate data in the high-angle region and reliable intensities of weak reflections are required. Both goals can best be achieved by the use of SR.

Experimental

Intensities were collected at the five-circle diffractometer of HASYLAB (DESY, Hamburg, Germany) (Kupcik, Wendschuh-Josties, Wolf & Wulf, 1986) while the storage ring DORIS II was operating in single-bunch mode under high-energy conditions at 5.3 GeV. During this mode – for HASYLAB users the so-called 'parasitic' mode – a typical run lasts about 50 min. The beam-position stabilization is switched off. The background is increased by photons of extremely high energy (> 80 keV) and at the same time the intensity is reduced as a result of a lower ring current compared with the dedicated (for HASYLAB users) operating mode. Kirfel & Eichhorn (1990) demonstrated that data obtained under these less favourable conditions are still superior to the sealed X-ray tube data, even for relatively large crystals.

The volume of our crystal is about 1/10 of that used by Gies (1986). The crystal was also used for the measurement of two additional data sets on an Enraf–Nonius CAD-4 diffractometer with monochromatized Mo $K\alpha$ radiation at room temperature and at 155 K. A second crystal from the same bunch but with double the volume was selected for long-exposure (up to 14 d) Weissenberg and precession photographs.

Details of the measurement procedure are presented in Wendschuh-Josties & Wulf (1989). The data extraction and analysis of the synchrotron data was performed using the package *CRYSTAL* especially written and adapted for SR data by Eichhorn (unpublished). After dead-time correction of the three counting chains (polarimeter and main counter), the window method of Grant & Gabe (1978) and a least-squares fit of the background were used to determine the integrated intensities from the profiles. A numerical correction for absorption was applied. Additional information is given in Table 1; for crystal data see Table 2. Laue group $P6/mmm$ is

Table 1. *Measurement conditions*

Monochromator	Flat double crystal Si(111) in $(+n, -n)$ arrangement
Wavelength (Å)	0.78914 (5)
Collimator diameter (mm)	1
Detector aperture (mm)	3 × 3
Sample–detector (mm)	248
Temperature (K)	293 (2)
Scan mode	ω scan, 101 steps, 0.005° each, 0.3–2.0 s step^{-1}
Standard reflection	$55\bar{9}$
Measured reflection	$\sin\theta/\lambda_{max} = 0.64$ Å^{-1} $0 \le h \le 15$, $0 \le k \le 15$, $-14 \le l \le 14$ (4 asymmetric units, 3130 reflections)
Unique reflections	845
>0	784
$\ge 2\sigma(F)$	736
$R_{int}(I)$ after averaging	0.028

Table 2. *Crystal data*

Formula (content of the unit cell)	$34SiO_2(C_{10}H_{15}NH_2)5NH_3$
Space group	*P6/mmm*
Lattice constants	
At 293 K a, c (Å), V (Å^3)	13.826 (3), 11.186 (3), 18521 (1)
At 155 K a, c (Å), V (Å^3)	13.748 (3), 11.128 (3), 1821 (1)
$F(000)$	1154
D_x at 293 K (g cm^{-3})	2.043
Crystal shape and size (mm)	Hexagon plate, thickness 0.013, side of hexagon 0.075
V (μm^3)	2×10^5
Absorption coefficient (cm^{-1})	8.51
Minimum, maximum transmission	0.911, 0.989

confirmed by the internal R value, hence possible space groups are *P6/mmm*, *P$\bar{6}$m2*, *P$\bar{6}$2m*, *P6mm* and *P622*. Weissenberg and precession photographs did not give any indication of diffuse intensities or superstructures.

Mosaicity

Because of the high parallelity of the monochromatic X-ray beam the shape of the ω-scanned reflection profiles is governed by the mosaicity of the crystal. Fig. 1 displays the dependence of the profiles on χ and φ. The full width of the base (say 1/10 width) changes considerably indicating a non-isotropic orientational distribution of the mosaic blocks, but never exceeds $\Delta\omega = 0.2°$. The half width of a reflection from a single block can be estimated to be in the order of $\Delta\omega \simeq 0.01°$.

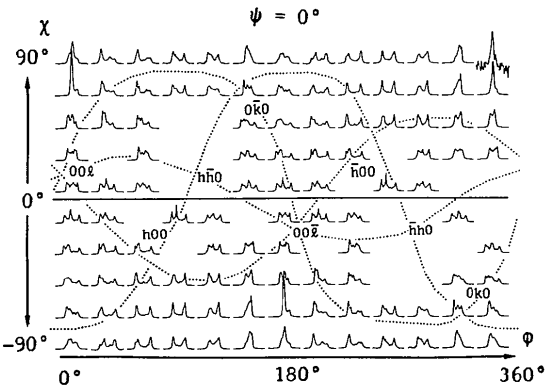

Fig. 1. ω-scanned reflection profiles in the χ,φ plane at $\psi = 0°$ with the orientation matrix used for measurement. Figured range $\Delta\omega = 0.3°$. Normalized to equal integrated intensity. $\chi = -90°$ corresponds to $hkl \simeq 3\ 8\ \bar{3}$.

The block structure becomes more evident in Fig. 2, which allows the trace of single blocks or groups of orientationally related blocks during ψ scans of single reflections to be followed.

On the one hand these features hamper the determination of a precise orientation matrix and hence of precise lattice constants, and they impose a small stepwidth during data collection. On the other hand they enable us to analyse the mosaicity of the crystal. An analysis of the block structure based on all measured profiles shows that the anisotropy of the orientational distribution of the mosaic blocks is not correlated with any prominent crystallographic direction.

Refinement of the host structure

The anisotropic refinement with *SHELX*76 (Sheldrick, 1976) in space group *P6/mmm* starting with the coordinates of Gies (1986) led to parameters most of which agree with the parameters of Gies within 2σ. This is valid even for the components of the U_{ij} tensors. Weights proportional to $1/\sigma^2(F)$ were applied. After a rigid-body refinement of the 1-aminoadamantane molecule the threefold axis of which was assumed initially to coincide with the sixfold axis of the $5^{12}6^8$ cage ($wR = 4.0\%$) the residual electron density was concentrated at the O atom sites and clearly indicated a splitting of these positions (Fig. 3*b*). The Si atoms did not reveal any features. The Fourier section Fig. 3(*a*) shows the non-spherical shape of the electron density at the O-atom positions.

Besides our finding that the Si-atom positions have 'normal' and nearly isotropic a.d.p.'s the assumption that the Si atoms are not disordered is supported by the results of ^{29}Si NMR measurements of D1H (Groenen, Alma, Dorrepaal, Hays & Kortbeek, 1985) which reveal the expected four independent Si-atom positions.

The results concerning the simultaneously refined guest molecules are discussed later in this paper.

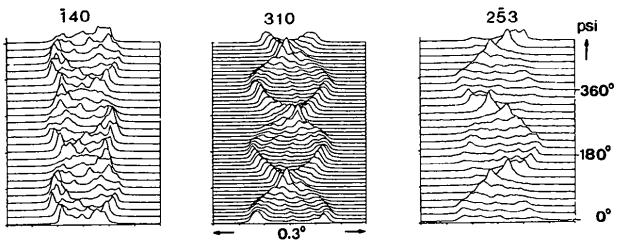

Fig. 2. ψ scans for three selected reflections; horizontal axis is ω.

The additional degrees of freedom obtained when one of the space groups $P\bar{6}m2$, $P\bar{6}2m$, $P6mm$ or $P622$ is used to describe the structure cannot solve the problem of splitting. The pronounced splitting of O(7) (Fig. 3*b*) indicates the lack of the threefold axis. Consequently, none of the refinements in these space groups gave a conclusive result. To avoid the complications and instabilities connected with highly correlated parameters and the loss of the inversion centre, *P6/mmm* was used in the following calculations.

The O-atom positions were split into two to four positions by removing the atoms from special positions and/or introducing new sites. These split positions were refinable without constraints. The amount of splitting is about 0.5 Å, the mean U_{eq} decreased to about 0.037 Å^2, wR dropped from 4.0 to 1.75%. The Si—O distances ranged from 1.56 to 1.63 Å, the mean value being 1.60 Å. The σ's of the positional parameters became rather large (123 variables for the host lattice). Therefore soft constraints for Si—O distances: d(Si—O) = 1.60 ± 0.03 Å were introduced to fix the O atoms in a plane perpendicular to the Si—Si direction and halfway between the two Si atoms. After a few cycles the refinement led to wR = 1.76% with an 'improved' geometry. The residual electron density disappeared only when anisotropic U's were used. Only the symmetry-conditioned constraints between the components of the U_{ij} tensor were applied. The distribution of the population parameters on the split sites became well equilibrated.

The Si—O—Si angles in the split model range from 147 to 165°, the Si—O distances are distributed between 1.58 and 1.61 Å which, of course, is a consequence of the constraints.

Fig. 4 compares the results of refinement with and without splitting. The reasonably shaped thermal ellipsoids of the split O atoms illustrate the remark-

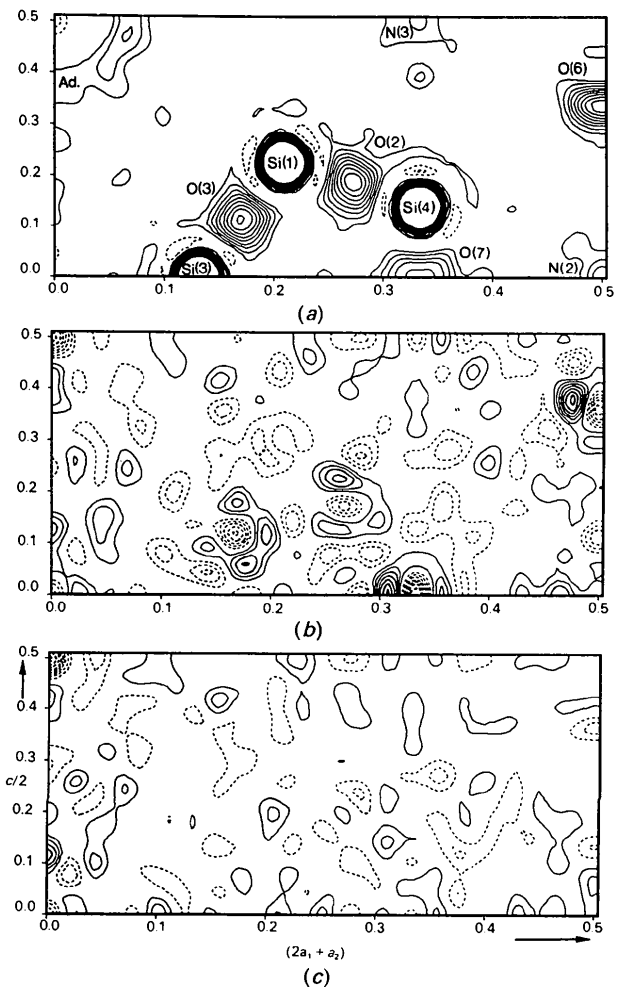

Fig. 3. Fourier and difference Fourier syntheses, zero contours omitted for clarity. (*a*) Fourier section, contours 1.0 e Å^{-3}. (*b*) difference Fourier section, anisotropic refinement, contours 0.1 e Å^{-3}, (*c*) As (*b*), O atoms split.

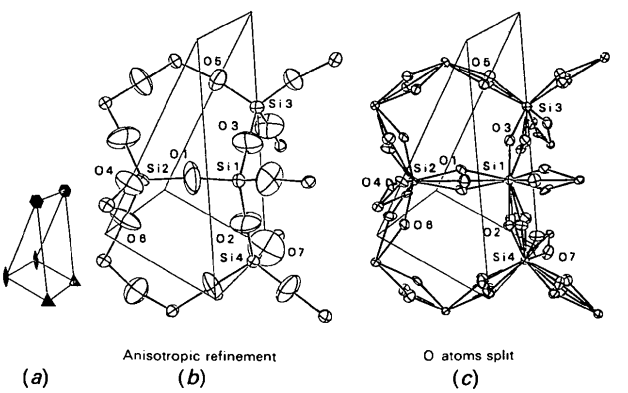

Fig. 4. Asymmetric unit of D1H: (*a*) position of symmetry elements; (*b*) anisotropic refinement, 50% probability; (*c*) O atoms split, 20% probability.

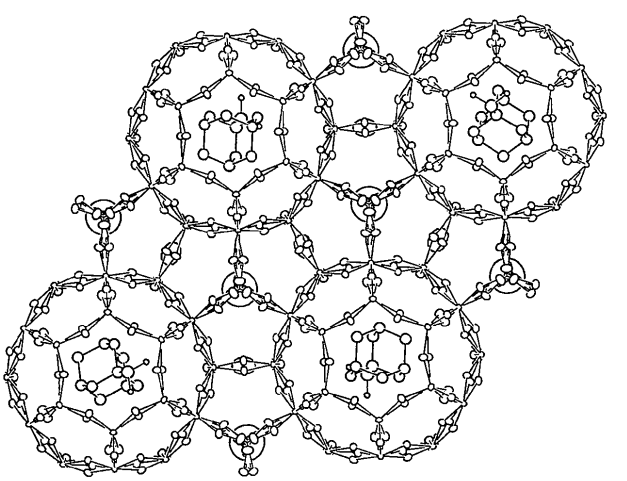

Fig. 5. The crystal structure of D1H projected down **c**. Split O-atom sites, guest molecules included.

Table 3. *Atomic coordinates and equivalent isotropic displacement parameters* (Å^2)

Thermal factors have the form $\exp[-2\pi^2 U_{eq}(\sin\theta/\lambda)^2]$.

	x	y	z	K	U_{eq}
SiO_2 framework					
Si(1)	0.41830 (4)	0.20915 (2)	0.22520 (4)	$\frac{1}{2}$	0.0194 (2)
Si(2)	0.38754 (4)	0	0.36188 (4)	$\frac{1}{2}$	0.0185 (3)
Si(3)	0.26248 (6)	0.13124 (3)	0	$\frac{1}{4}$	0.0215 (3)
Si(4)	$\frac{2}{3}$	$\frac{1}{3}$	0.13871 (8)	$\frac{1}{6}$	0.0196 (4)
O(1,1)	0.429 (1)	0.115 (1)	0.294 (2)	0.210 (7)	0.038 (5)
O(1,2)	0.3747 (7)	0.885 (5)	0.2837 (7)	0.376 (7)	0.031 (2)
O(1,3)	0.3972 (9)	0.1162 (6)	0.3222 (5)	0.495 (7)	0.039 (2)
O(2,1)	0.5492 (7)	0.264 (2)	0.2074 (6)	0.248 (6)	0.036 (4)
O(2,2)	0.5395 (6)	0.251 (1)	0.1653 (6)	0.303 (6)	0.045 (3)
O(3,1)	0.362 (1)	0.1809 (6)	0.0954 (1)	0.103 (6)	0.032 (5)
O(3,2)	0.3342 (4)	0.1482 (5)	0.1187 (3)	0.452 (6)	0.040 (2)
O(4,1)	0.387 (2)	0.029 (2)	$\frac{1}{2}$	0.113 (6)	0.031 (4)
O(4,2)	0.3591 (8)	0	$\frac{1}{2}$	0.157 (6)	0.030 (4)
O(5,1)	0.192 (1)	0	0.023 (2)	0.168 (6)	0.042 (4)
O(5,2)	0.175 (2)	0	0	0.106 (6)	0.035 (5)
O(6)	0.9776 (4)	0.4888 (2)	0.3411 (2)	0.281 (2)	0.043 (3)
O(7)	0.6342 (5)	0.3171 (3)	0	0.092 (1)	0.048 (4)
NH_3					
N(2)	$\frac{1}{2}$	0	0	0.141 (2)	0.248 (7)
N(3,1)	0.636 (3)	0.318 (2)	$\frac{1}{2}$	0.052 (1)	0.265 (8)
N(3,2)	0.697 (3)	0.349 (2)	0.453 (2)	0.046 (1)	0.265 (8)
1-Aminoadamantane					
C(1)	0.101 (2)	0.117 (2)	0.597 (3)	0.0460 (2)	0.110 (8)
C(2)	0.138 (1)	0.051 (2)	0.516 (2)		
C(3)	0.101 (1)	0.057 (3)	0.387 (2)		
C(4)	−0.028 (2)	0.000 (2)	0.384 (2)		
C(5)	−0.027 (2)	0.062 (2)	0.595 (2)		
C(6)	−0.067 (2)	0.063 (3)	0.467 (2)		
C(7)	−0.080 (2)	−0.059 (2)	0.640 (2)		
C(8)	0.084 (3)	−0.072 (2)	0.559 (3)		
C(9)	−0.045 (2)	−0.126 (2)	0.557 (2)		
C(10)	−0.079 (2)	−0.122 (2)	0.426 (2)		
N(1)	−0.064 (2)	0.002 (3)	0.261 (1)	0.0460 (2)	0.180 (9)

able numerical stability of the refinement process. Fig. 5 shows the complete unit cell. The guest molecules are given in their final orientation which is discussed later on.

Table 3 briefly compares conditions and results for the refinements with and without splitting. For the guest molecules in the anisotropic refinement the final parameters from the refinement of the split model (Table 4) were used.*

Population parameters of O atoms

When allowed to refine freely the population parameters K of the O atoms increased without exception and all by about the same amount. The average values of K are 1.149 for isotropic, 1.112 for anisotropic refinement, and 1.095 for $\sum K$ of the split O-atom positions. The use of scattering curves for Si^{2+} and O^- instead of those for neutral Si and O has only a very minor effect.

If an anisotropic refinement is performed with synthetic structure factors from a model structure with split sites instead of experimental data the same phenomenon can be observed. The idea that this artefact is connected in any way with the fact that the least-squares algorithm minimizes the sum of squared deviations is supported by model calculations which are easy to survey and described in more detail in the *Appendix*.

Table 4. *Comparison of anisotropic and split models*

	Anisotropic model	Split model
R, wR (%)	4.74, 3.87	2.61, 1.76
Free parameters (host framework)	55	123
Free parameters* (guest molecules)	92	92
Free parameters	147	215
Mean Si—O (Å)	1.568	1.596 (11)
Mean ∠Si—O—Si (°)	170.5	155 (3)
U_{eq} (Å^2) (oxygen)	0.065	0.038 (6)

* Including hydrogen, soft constraints applied.

Results from conventional 155 K and room-temperature data

In order to separate the dynamic contribution of the anisotropic displacement parameters, data collection using the same crystal as for SR data collection was performed at 155 K using an Enraf–Nonius CAD-4 diffractometer with Mo $K\alpha$ radiation. Though the quality of these data is not comparable with the SR data ($R = 12.5\%$, $wR = 8.3\%$ for the anisotropic refinement of the non-split O atoms) the following results were obtained: (i) again Laue symmetry $P6/mmm$ is confirmed, $a = 23.748$ (3), $c = 11.128$ (3) Å; (ii) there is an average decrease of 14% for the a.d.p.'s of Si. For the non-split O atoms the a.d.p. component in the direction of the Si—O bond decreases about 30% while the average decrease perpendicular to this direction is only 12% so that the anisotropy is even more accentuated than in the room-temperature structure.

Under the same conditions a data collection was performed at room temperature. The parameters obtained from a refinement of these data with non-split anisotropic O atoms coincide with the results from SR data within 1σ limits, $R = 6.7\%$, $wR = 3.7\%$. The comparatively low wR is obtained as a result of the low weights of the weak reflections. Some indications for splitting can be recognized in the difference synthesis but they barely exceed the level of noise (Fig. 6). An attempt to refine split O-atom positions failed because of numerical problems caused by extremely high correlations. A comparison of the quality of data and models expressed by the dependence of the R factors on $\sin\theta/\lambda$ is given in Fig. 7. This comparison, however, is slightly unfair since the conditions for the Mo $K\alpha$ data collection were not optimized with the same effort as used for the SR data collection.

* Lists of structure factors, anisotropic thermal parameters and H-atom parameters have been deposited with the British Library Document Supply Centre as Supplementary Publication No. SUP 55961 (11 pp.). Copies may be obtained through The Technical Editor, International Union of Crystallography, 5 Abbey Square, Chester CH1 2HU, England. [CIF reference SH0023]

Distance least-squares calculations

The way in which the topology of the SiO_2 framework of D1H could accommodate the measured lattice constants if some or all symmetry constraints except translational symmetry are withdrawn was checked by a distance least-squares procedure.

Two considerations were made when planning the strategy:

(I) *Translationengleiche* subgroups of *P6/mmm* should not contain two- or threefold axes parallel to **c**. This condition is suggested by the observed splitting of O(6) and O(7), respectively. The subgroups should neither have a twofold axis perpendicular to **c** [this follows from the splitting of O(4) and O(7)] nor a mirror plane perpendicular to **c** [this follows from the splitting of O(2), O(3), O(4) and O(5)]. Therefore all hexagonal, trigonal, orthorhombic and most of the monoclinic subgroups are excluded. Hence the calculations were done in the most general space group *P*1, transformed to the 'orthohexagonal' setting *C*1 to minimize correlations between the positional parameters.

(II) The calculated Si positions should not essentially deviate from the observed ones. This condition is suggested by the results of structure refinement and is essentially equivalent with the assumption that the more or less rigid SiO_4 tetrahedra are merely allowed to librate around their fixed centres of mass which coincide with the Si atoms.

The calculations were performed with the program *DLS*76 (Baerlocher, Hepp & Meier, 1977). Two groups of calculations in space group *C*1 were performed: one group with 101 atoms [=(Si + O) content of the asymmetric unit minus one origin-defining atom] free, and, to account for consideration (II), a second group with all Si atoms fixed at the positions from structure refinement and 68 O atoms free.

A total of 200 starting sets with free positional parameters generated by a Monte Carlo procedure

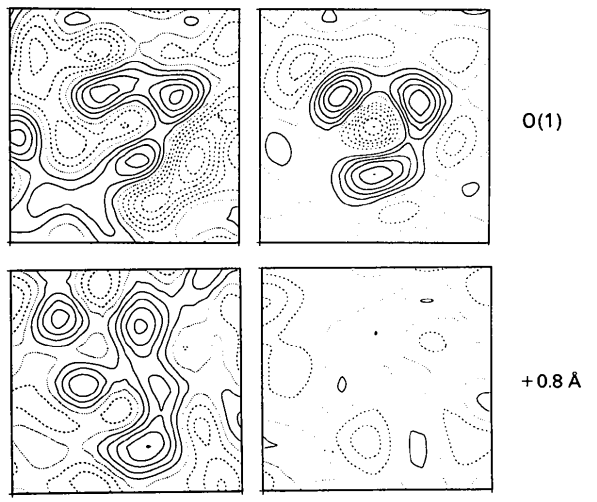

Fig. 6. Mo $K\alpha$ data *versus* SR data. Difference Fourier sections through two planes perpendicular to the Si(1)—Si(2) direction. Contours 0.1 e Å^{-3}, edge of the squares: 3 Å. Above: section through O(1), below: 0.8 Å below O(1). Left-hand side: Mo $K\alpha$, right-hand side: SR.

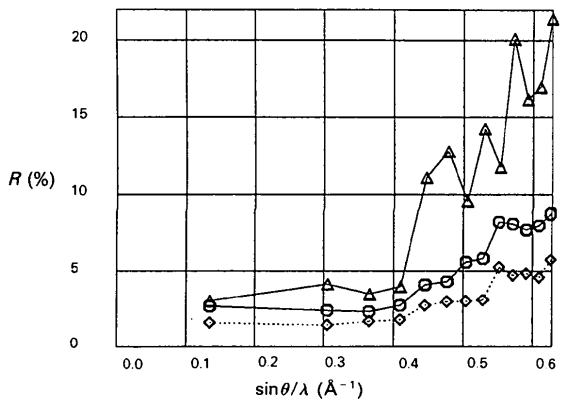

Fig. 7. Variation of the *R* factor with $\sin\theta/\lambda$. Each point calculated from *ca* 60 reflections. ◇: SR data, O atoms split; ○: SR data, anisotropic refinement without splitting; △: Mo $K\alpha$ data, parameters as ◇.

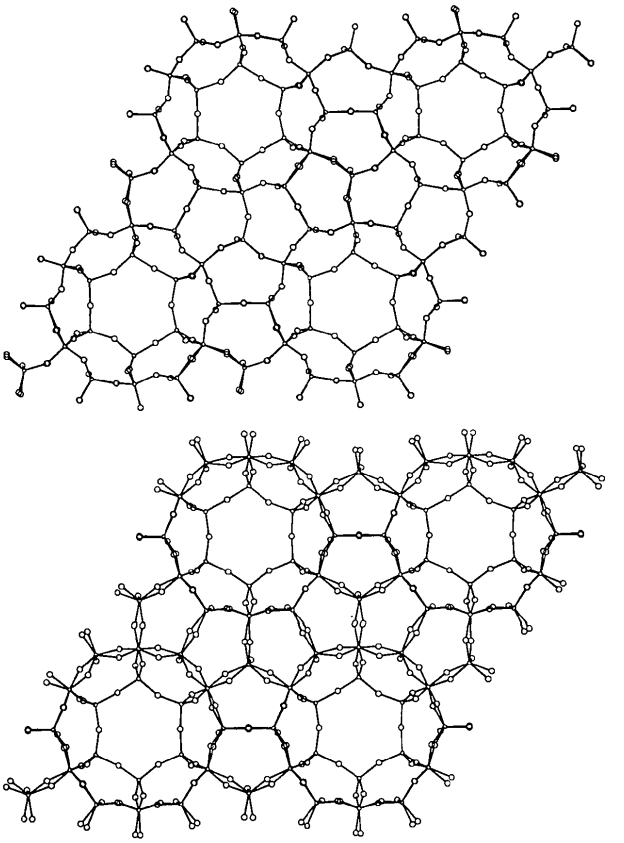

Fig. 8. Two typical *DLS* solutions displaying space group *P*1. Si atoms fixed, prescribed values: *d*(Si—O) 1.60 Å, angle (Si—O—Si) 150°.

were refined. Different groups of starting sets were given different prescribed values for Si—O distances and Si—O—Si angles and different weights for these values. The large number of starting sets allows for a statistical discussion of general trends.

All runs with free Si atoms automatically generated structures with symmetries higher than $P1$: $P6/m$, $P\bar{3}$, $P112/m$ and $P\bar{1}$. The relative abundance of these space groups depends on weights and prescribed distances and angles. Among these solutions only those with space group $P\bar{1}$ are consistent with consideration (I), but they strongly distort the silicon sublattice and hence violate the precondition made in consideration (II).

Models which are consistent with considerations (I) and (II) were generated only with fixed Si-atom positions: besides some solutions with hexagonal symmetry – which again are inconsistent with consideration (I) – the majority of models displayed symmetry $P1$ ($C1$), frequently close to configurations of higher symmetry. Two typical solutions are given in Fig. 8.

The O-atom distributions as shown on the left-hand side of Fig. 9 were obtained by applying the symmetry operations of $P6/mmm$ to all atoms of the *DLS* solutions of Fig. 8. Positions closer than 0.1 Å were merged. The similarity with the result of refinement is evident.

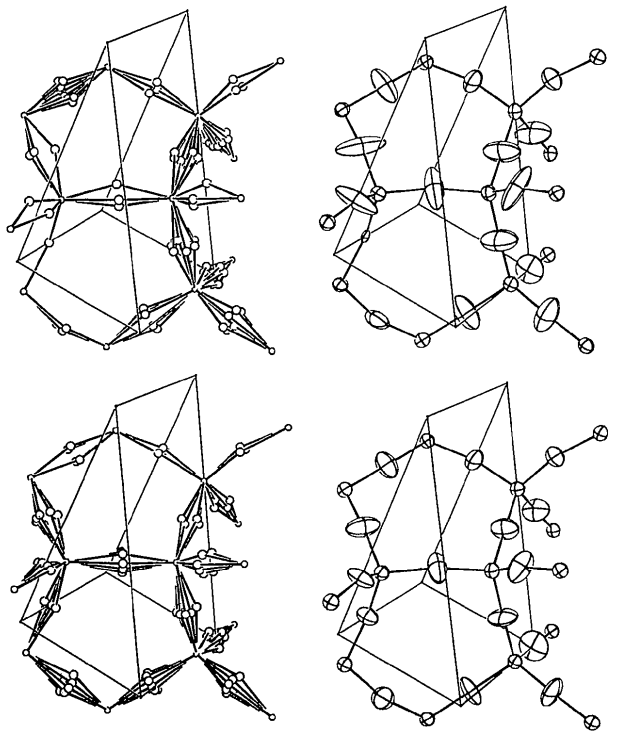

Fig. 9. Left side: the $P1$ structures of Fig. 8, convoluted by the symmetry elements of space group $P6/mmm$, asymmetric unit. Right side: result of anisotropic refinement in space group $P6/mmm$ based on F_c of the $P1$ structures from Fig. 8 averaged in Laue group $P6/mmm$. Above: $R_{int}(F) = 10\%$; below: $R_{int}(F) = 12\%$.

Simulation of twinning and incomplete data sets

Having observed the mosaicity of the crystal in the ω scans we worried about the possibility of errors in our measured intensities caused by incoherent scattering from different individuals of lower symmetry.

Already the quite well defined and interpretable features at the O-atom positions in the difference Fourier synthesis seem to indicate that the high Laue symmetry $P6/mmm$ is not the result of an incoherent superposition of intensities from crystallites of lower symmetry. To investigate the effect of twinning and partial data sets on the result of the least-squares refinement, model calculations were performed.

Intensities for a full sphere up to $\sin\theta/\lambda = 0.64$ Å^{-1} – the value of the experiment – were calculated for different $P1$ structures resulting from *DLS* runs. Isotropic thermal parameters $U(\text{Si}) = 0.02$, $U(\text{O}) = 0.023$ Å^2 were used.

To simulate balanced twinning one group of data sets was generated by averaging the intensities in Laue group $P6/mmm$ which led to $R_{int}(I) = 0.10$ and 0.12 for the two models of Fig. 8. In order to simulate incomplete data sets a second set was obtained by extracting groups of reflections which correspond to randomly chosen asymmetric units of Laue group $P6/mmm$ in reciprocal space.

If one compares the results of anisotropic refinement of the structures in $P6/mmm$ based on these data sets with the shape of the corresponding hexagonally averaged triclinic structures (*e.g.* Fig. 9 for balanced twinning) a remarkable correlation can be observed despite the introduced errors. Especially the Si atoms remain nearly isotropic with $U = 0.02$ Å^2.

From this result an incoherent superposition of intensities as well as the use of an incomplete data set might be a possible source of the large a.d.p.'s of the O atoms and their anisotropy. But in contrast to the refinement with our experimental data, difference Fourier maps do not reveal any clear features at the O-atom positions.

Discussion

Host framework

There are some considerations to be taken into account when judging the evidence of the positional parameters of the O atoms obtained from the structure refinement:

(1) Soft constraints for Si—O distances had to be used to enforce a 'good' geometry of the host framework. The average distance of the split O atoms is about 0.5 Å with and without constraints.

(2) The U's of the split O atoms are handled anisotropically, even then the sum of the population parameters of the split sites is still greater than 1.0. This is one more indication that the configuration of the O atoms obtained from refinement is not a description of 'the whole truth'.

With the positional parameters given in Table 4 it is not possible to find a model with the periodicity of the unit cell that fits both angles and distances within the limits given by 'normal' silica phases. However, it is not to be expected that such a possibility exists: from the model calculations we conclude that Laue symmetry *P6/mmm* is really present, at least at the time resolution of an X-ray experiment, and that this Laue symmetry is not the result of incoherent superposition of intensities from individuals with lower symmetry.

The following qualitative considerations are to be seen as a possible explanation of the disordered state of the host framework.

It is noticeable that in D1H – as well as in D3C – all pairs of linked SiO_4 tetrahedra are arranged in a *cis* configuration, *i.e.* two linked tetrahedra transform into each other by a (local) mirror plane through the linking O atom. The structure of β-tridymite is governed by this configuration. In D1H the *cis* configuration is enforced by global mirror planes for all pairs of tetrahedra except for the group $Si(1)Si(2)O_7$ where the mirror plane is local.

Since the presence of the large guest molecules is a precondition for the growth of dodecasil crystals from the solution it can be assumed that the formation of the cages around these molecules is an elementary step at the beginning of crystallization. Here the *cis* arrangement of the SiO_4 tetrahedra is favourable since it leads to smooth 'interior walls' of the cages around the voluminous and electrically neutral molecules.

On the other hand, for an isolated Si_2O_7 group the *cis* configuration is known to be energetically less favourable than the *trans* configuration which contains a (pseudo) inversion centre in the linking O atom.

The contradiction between these two tendencies might be a reason for the latent instability of the dodecasil structures.

Guest molecules

All cages are fully occupied: the 5^{12} and $4^3 5^6 6^3$ cages by NH_3 and the $5^{12}6^8$ cage by 1-aminoadamantane molecules. All guest molecules are strongly disordered. U_{eq} is 0.27 Å^2 for the NH_3 molecule in the 5^{12} cage [N(2)] and 0.20 Å^2 for the split sites [N(3,1), N(3,2)] in the $4^3 5^6 6^3$ cage. Sections through the difference densities representing the NH_3 molecules are given in Fig. 10.

Fig. 11 shows two sections through the difference electron density within the $5^{12}6^8$ cage when the 1-aminoadamantane molecule is excluded from the calculation of structure factors. The inset molecule suggests that the off-axis maximum at (0.06, 0, 0.26) is likely to be interpreted as the amino group. The N atom points towards the 3.2 Å distant atom O(5). The most probable orientation of the molecule which has point symmetry 3*m* does not accommodate any symmetry element of the 6/*mmm* symmetry of the cage (*cf.* also Fig. 5). The threefold axis of the molecule is *ca* 20° inclined with respect to the sixfold axis of the cage. A comparison of the upper and the lower part of Fig. 11 shows that the observed electron density is fairly well explained by the 24 overlapping orientations of the molecule.

Because of the high $\bar{4}3m$ symmetry of the adamantane nucleus the orientation of the molecule is essentially defined by the orientation of the amino group. For a strongly librating molecule and an angle near 90° between the sixfold axis and the direction of the C—NH_2 bond, the electron density of the amino group would be smeared out over a large volume and hence scarcely detectable. There-

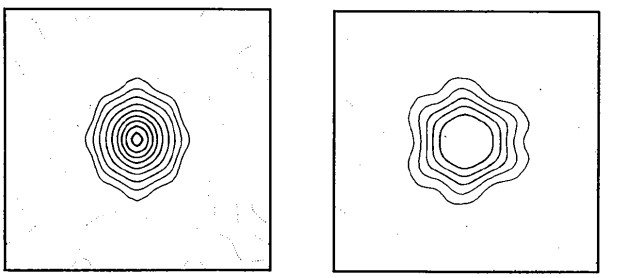

Fig. 10. Difference Fourier section through $N(2)H_3$ (left) and $N(3)H_3$ (right). F_c without the corresponding molecules. Contours 0.25 e Å^{-3}, edge of the squares 6 Å.

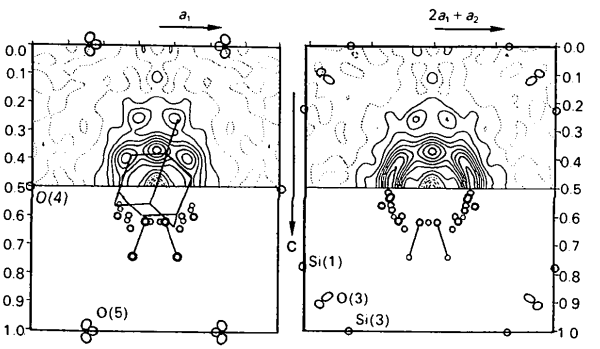

Fig. 11. Difference Fourier sections through the $5^{12}6^8$ cage containing the sixfold axis. F_c without 1-aminoadamantane; contours 0.25 e Å^{-3}. Circles in the lower half: atoms of the 24 overlapping molecules within a disc limited by the plane of the section and a plane 0.6 Å below, thickness of contours decreasing with increasing distance from the plane of section.

fore we cannot exclude the presence of a secondary orientation of this type.

Concluding remarks

For the problem under investigation the required reliability of intensities of the weak reflections makes synchrotron data – even when collected under non-optimum conditions – superior to those measured with conventional X-ray tubes. The features connected with the splitting of O atoms require a good resolution in direct space. They can be interpreted only when the contribution of the generally weaker high-order reflections – which determine the resolving power of the diffraction experiment – is not obscured by noise from inaccurate data. Furthermore, the good quality of data causes a remarkable numerical stability of the least-squares procedure when highly correlated parameters are simultaneously refined.

The experimentally determined deviations of the O-atom positions from their averaged sites are in good agreement with the local perturbation of the structure as derived from *DLS* simulations. Artefacts introduced by incoherent superposition of intensities from merohedral twins and/or from an incomplete data set can be excluded as shown by model calculations. Since no indication for a superstructure was found we conclude that the perturbations are non-periodic.

The temperature dependence of the a.d.p.'s resulting from anisotropic refinement without splitting seems to indicate that the perturbations of this structure are static. On the other hand the fact that the Si atoms are not affected by the disorder is not satisfactory explained by this assumption. Further spectroscopic investigations as a function of temperature are required to elucidate the behaviour of the SiO_2 framework.

APPENDIX

Population parameters of disordered atoms, a semiempirical approach

The anisotropic refinement of the disordered O-atom sites in D1H without splitting leads to a mean U_{eq} of 0.065 Å^2 and $R = 0.047$, $wR = 0.038$. If the population parameters of the O atoms are refined they increase to an average value of $K = 1.11$. The mean U_{eq} increases to 0.73 Å^2 with $R = 0.039$ and $wR = 0.031$. The improvement in R is reflected by a distinct reduction of the positive and negative residual electron density at the O-atom positions.

This behaviour can be reproduced if structure factors calculated from a model structure with split sites are used instead of experimental data. The effect

Table 5. *K and U obtained from the refinement of model structures* 1 *and* 2

	x(O)	d (Å)*	K(O)		U_{11}		U_{33}
Model:	1, 2	1, 2	1	2	1	2	1, 2
	$\frac{1}{3}$	0.0	1.0		0.02		0.02
	0.325	0.199	1.005	1.005	0.042	0.042	0.020
	0.321	0.294	1.021	1.023	0.073	0.075	0.020
	0.317	0.390	1.043	1.052	0.122	0.130	0.020
	0.313	0.485	1.056	1.087	0.185	0.201	0.020

* Distance O(model) – ($\frac{1}{3}$, $\frac{2}{3}$, 0).

is obviously inherent in the least-squares algorithm when the electron density of a split site is described by a single atom.

The magnitude of the effect depends on many parameters, such as K, U, relative abundance and Z of split and non-split atoms, symmetry situation *etc.*

Table 5 gives the dependence of K and U on the amount of splitting for two simple model structures: lattice constants and space group as D1H, data calculated up to $(\sin\theta/\lambda)_{max} = 0.64$ Å^{-1} for

Si at ($\frac{1}{3}$, $\frac{2}{3}$, 0.13865),

$$U = 0.02 \text{ Å}^2, \quad K = 1 \text{ (model 1)}, \quad K = 2 \text{ (model 2)}$$

O at (x, $2x$, 0),

$$U = 0.02 \text{ Å}^2, \quad K = 1 \text{ (models 1 and 2)}$$

During refinement x(O) was fixed.

A rough approach to this artefact is to assume that the minimization of

$$\sum w[F_{obs}(h) - F_{calc}(h)]^2$$

is equivalent to the minimalization of

$$\int[\rho_{obs}(x) - \rho_{calc}(x)]^2 dx \qquad (1)$$

and to compare $\int\rho_{obs}dx$ and $\int\rho_{calc}dx$ after minimalization of (1).

To describe $\rho_{obs}(x)$ we use symmetrical one-dimensional functions

$$\rho_n(x) = [(2^{1/n} - 1)x^2 + 1]^{-n} \qquad (2)$$

($n = 1$: Lorentz, $n = \infty$: Gauss, FWHM = 2)

The splitting of a site into two sites with the distance x_0 is modelled by the function

$$f_n(x;x_0) = \tfrac{1}{2}[\rho_n(x - \tfrac{1}{2}x_0) + \rho_n(x + \tfrac{1}{2}x_0)].$$

Then the parameters a and b of the function

$$g_n(x;a,b) = a\rho_n(x/b),$$

are fitted to minimize

$$\int_{-\infty}^{\infty} [f_n(x,x_0) - g_n(x;a,b)]^2 dx.$$

The parameter a is the maximum value of $g(x;a,b)$, b is correlated with the half width of the modelled distribution and hence correlated with the a.d.p.

Table 6. *Values of* $\Delta_n(x_0)$ [*cf. definition* (3)]

$\frac{1}{2}x_0$ is the ratio (amount of splitting)/full width at half maximum.

		$\frac{1}{2}x_0$: 0.15	0.3	0.6	0.9
Lorentz	$n=1$	1.0055	1.0210	1.0710	1.1270
	2	1.0028	1.0109	1.0395	1.0747
	4	1.0014	1.0059	1.0245	1.0509
	8	1.00076	1.0034	1.0173	1.0402
	16	1.00041	1.0022	1.0138	1.0354
	32	1.00024	1.0015	1.0121	1.0335
Gauss	∞	1.00007	1.0009	1.0105	1.0309

It can be shown that under these conditions always

$$\int_{-\infty}^{\infty} g_n^2(x;a,b)\mathrm{d}x \Big/ \int_{-\infty}^{\infty} f_n^2(x;x_0)\mathrm{d}x \le 1$$

but a general statement on the behaviour of

$$\Delta_n(x_0) = \int_{-\infty}^{\infty} g_n(x;a,b)\mathrm{d}x \Big/ \int_{-\infty}^{\infty} f_n(x;x_0)\mathrm{d}x, \qquad (3)$$

which is our quantity of interest, is not possible. $\Delta_n(x_0)$ may be considered as the calculated population parameter and should be 1. Obviously it is 1 for $x_0 = 0$.

The numerical evaluation of the least-squares fit shows that $\Delta_n(x_0)$ increases with increasing x_0, at least for the functions of type (2). For functions $\rho(x)$ with very steep flanks such as $\rho(x) = \exp(-|x|^z)$ with $z > 2$ the increase of Δ with increasing x_0 is preceded by a narrow x_0 range with $\Delta < 1$.

Table 6 lists values of Δ_n as function of n and x_0. In three dimensions, $(\Delta - 1)$ should be about three times as large. Then the magnitude of order of Δ is comparable with the observed effect.

Support of this work by the Bundesminister für Forschung und Technologie (grant 03-FU2DAR) is gratefully acknowledged.

References

ANDREWS, S. J., PAPIZ, M. Z., MCMEEKING, R., BLAKE, A. J., LOWE, B. M., FRANKLIN, K. R., HELLIWELL, J. R. & HARDING, M. M. (1988). *Acta Cryst.* **B44**, 73–77.

BAERLOCHER, C., HEPP, A. & MEIER, W. M. (1977). *DLS76 Manual.* Institut für Kristallographie und Petrographie, ETH, Zürich.

FREIMANN, R. & KÜPPERS, H. (1991). *Phys. Status Solidi*, **123**, K123–K127.

GERKE, H. & GIES, H. (1984). *Z. Kristallogr.* **166**, 11–22.

GIES, H. (1986). *J. Incl. Phenom.* **4**, 85–91.

GRANT, D. F. & GABE, E. J. (1978). *J. Appl. Cryst.* **11**, 114–140.

GROENEN, E. J. J., ALMA, N. C. M., DORREPAAL, G. R., HAYS, G. R. & KORTBEEK, A. G. T. G. (1985). *Zeolites*, **5**, 361–363.

KIRFEL, A. & EICHHORN, K. (1990). *Acta Cryst.* A**46**, 271–284.

KÖNNECKE, M., MIEHE, G. & FUESS, H. (1992). *Z. Kristallogr.* **201**, 147–155.

KUPCIK, V. (1988). *Z. Kristallogr.* **185**, 673.

KUPCIK, V., WENDSCHUH-JOSTIES, M., WOLF, A. & WULF, R. (1986). *Nucl. Instrum. Methods*, **246**, 624–626.

LIEBAU, F. (1984). *Acta Cryst.* A**40**, C-254.

MIEHE, G., VOGT, T., MÜLLER, U. & FUESS, H. (1990). *Acta Cryst.* A**46**, C-172.

RIECK, W., EULER, H., SCHULZ, H. & SCHILDKAMP, W. (1988). *Acta Cryst.* A**44**, 1099–1101.

SHELDRICK, G. M. (1976). *SHELX76*. Program for crystal structure determination. Univ. of Cambridge, England.

WENDSCHUH-JOSTIES, M. & WULF, R. J. (1989). *J. Appl. Cryst.* **12**, 382–383.

Acta Cryst. (1993). B**49**, 754–760

Crystal Structure Correlations in the Photochemistry of Dimethyl 9-Phenyl-9,10-dihydro-9,10-ethenoanthracene-11,12-dicarboxylate

BY PHANI RAJ POKKULURI, JOHN R. SCHEFFER AND JAMES TROTTER

Department of Chemistry, University of British Columbia, Vancouver, BC, Canada V6T 1Z1

(*Received* 16 *August* 1992; *accepted* 1 *February* 1993)

Abstract

A study of the photochemistry of the title 9-phenyldibenzobarrelene-11,12-diester (1) reveals the formation of a semibullvalene derivative, dimethyl 8b-phenyl-4b,8b,8c,8d-tetrahydrodibenzo[*a,f*]cyclopropa[*cd*]pentalene-8c,8d-dicarboxylate (2), in acetone solution, with an additional cyclooctatetraene (COT) photoproduct, dimethyl 5-phenyldibenzo[*a,e*]cyclooctene-6,12-dicarboxylate (3), in acetonitrile, benzene and in solid-state photolysis. Crystal data: T = 294 K, Cu $K\alpha$, $\lambda = 1.5418$ Å, $C_{26}H_{20}O_4$, M_r = 396.44. (1), triclinic, $P\bar{1}$, $a = 10.713$ (1), $b = 11.991$ (1), $c = 8.177$ (1) Å, $\alpha = 95.71$ (1), $\beta = 105.14$ (1), $\gamma = 79.61$ (1)°, $V = 995.9$ (2) Å^3, $Z = 2$, $D_x = 1.322$ g cm^{-3}, $F(000) = 416$, $\mu = 6.8$ cm^{-1}, $R = 0.060$ for 3069 reflections. (2), monoclinic, $P2_1/n$, $a = 10.206$ (3), $b = 16.485$ (1), $c = 11.758$ (4) Å, $\beta = 95.48$ (2)°, $V = 1969.2$ (8) Å^3, $Z = 4$, $D_x = 1.337$ g cm^{-3}, $F(000) = 832$, $\mu = 6.9$ cm^{-1}, $R = 0.039$ for 2882 reflections. (3), triclinic, $P\bar{1}$, $a = 11.074$ (2), $b = 25.298$ (6), $c = 7.668$ (2) Å, $\alpha = 94.22$ (2), $\beta =$